Atomic Spectroscopy

Article

Contribution of Planetary Ball Milling to the Homogeneity of Pyrrhotite Reference Material for LA-ICP-MS

A. O. Klimov, [a] A. Bakhadur, [b] V. D. Abramova, [c] L. V. Ragozin, [a] and K. A. Kokh [a,b,*]

[a] Sobolev Institute of Geology and Mineralogy SB RAS, Novosibirsk, Russia

[b] Al-Farabi Kazakh National University, Almaty, Republic of Kazakhstan

[c] Institute of Geology of Ore Deposits, Petrography, Mineralogy and Geochemistry RAS, Moscow, Russia

Received: *August 06, 2025;* ***Revised:*** *September 08, 2025;* ***Accepted:*** *September 09, 2025;* ***Available online:*** *September 09, 2025.*

DOI: 10.46770/AS.2025.145

ABSTRACT: The present study optimized the planetary ball milling of synthetic pyrrhotite doped with trace metals in order to enhance homogeneity. It has been demonstrated that milling at 400 rpm with acetone is an effective method of reducing particle size, whilst also preventing oxidation and secondary phase formation, in contrast to the process of dry grinding. Annealed samples demonstrated excellent trace element uniformity (RSD ~2-3%) by LA-ICP-MS, comparable to or superior to existing standards. The work underlines the pivotal role of milling conditions in the production of reliable sulfide standards, which are essential for accurate analysis in geochemistry and materials science.

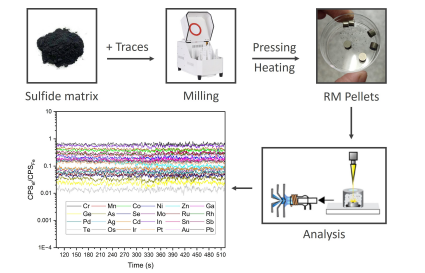

INTRODUCTION

Laser ablation inductively coupled plasma mass spectrometry (LA-ICP-MS) has become a powerful and widely used tool for the in-situ analysis of sulfide phases in geochemistry, mineralogy, and mineral processing. Its ability to achieve low detection limits, high spatial resolution, and rapid multi-element analysis makes it particularly suited for characterizing trace-element deportment — especially for economically critical metals such as platinum-group elements (PGEs), Au, Ge, and Ga, which often occur at ultra-low concentrations either in solid solution or as micro-inclusions within sulfides. Understanding their precise host phases and spatial distribution is essential not only for reconstructing ore-forming processes but also for designing efficient metallurgical flowsheets to maximize recovery[1] or minimize deleterious element content (*e.g.*, As, Hg). Pyrrhotite ($Fe_{1-x}S$), a common and reactive sulfide in many base- and precious-metal deposits, plays a pivotal role in these systems: it frequently hosts PGEs and other chalcophile elements, influences flotation behavior, and can act as a sink or carrier for trace metals during hydrothermal or metamorphic processes.[2] However, inaccurate calibration due to poorly characterized standards can lead to systematic under- or overestimation of element concentrations, potentially distorting interpretations of geological processes or misguiding decisions on the economic feasibility of ore deposit exploitation. [3]

The preparation of reliable LA-ICP-MS standards involves two major challenges: (1) achieving homogeneous distribution of trace impurities and (2) ensuring matrix compatibility with the analyzed samples. While femtosecond laser ablation has been shown to reduce matrix effects[4], the prevailing solution remains the development of sulfide reference materials with tailored compositions.[5–13] However, the synthesis of such standards involves complex methodologies with numerous poorly documented parameters.

In our previous work,[14] we demonstrated that post-synthesis annealing at 600°C significantly improves the homogeneity of trace-element distributions in synthetic pyrrhotite by promoting solid-state diffusion and eliminating metastable phases. However, that study relied on manual grinding in an agate mortar — a low-energy, non-standardized, and operator-dependent process that

inherently limits reproducibility and scalability. In this study, we introduce and systematically optimize a fully mechanized homogenization protocol using a planetary ball mill. Our results demonstrate that milling parameters (speed, duration, liquid medium) exert a decisive influence on achieving sub-micron-scale homogeneity while suppressing oxidation and phase segregation. This represents not merely an incremental improvement, but a methodological transition from artisanal sample preparation to a reproducible, instrument-controlled process — a necessary step toward the development of certified, inter-laboratory sulfide reference materials.

EXPERIMENTAL

Samples preparation. The pyrrhotite matrix — defined here as the pure Fe–S host phase prior to trace-element doping — was synthesized from elemental iron powder (4N) and elemental sulfur (4N). The reagents were placed within quartz ampoules, which were subsequently seales under vacuum 10^{-3} torr. The reagent weights were selected with the objective of producing pyrrhotite, which has the formula $Fe_{0.95}S$. After this, the ampoule containing the reagents was exposed to temperatures of 600°C for a period of 24 h. After the process of annealing, the ampoules were opened and the obtained pyrrhotite was ground in an agate mortar to a homogeneous powder. Subsequently, phase purity was verified through powder X-ray diffraction analysis.

Trace elements (Cr, Mn, Co, Ni, Cu, Zn, Ga, Ge, As, Se, Mo, Ru, Rh, Pd, Ag, Cd In, Sn, Sb, Te, Os, Ir, Pt, Au, and Pb) in the form of chalcogenides were introduced into the matrices in solid form at the stage of mechanical homogenization. The calculated concentration of elements was approximately 100 ppm for all elements except As (~44 ppm) and Se, Te (~800 ppm).

The mechanical homogenization of pyrrhotite powder with the source of traces was carried out in a SQM 0.4L planetary ball mill. Pyrrhotite powder weighing 2 g was placed in 0.1 L jars and 150 g of 5 mm diameter balls were added. The jars and balls were both made of zirconium oxide. Grinding was carried out using different regimes of operation of the ball mill. The ratio of the disk velocity to the pot velocity was 2:1. The revolution varied from 200 to 400 rpm, and the duration varied from 2 to 60 minutes. In some experiments, a liquid medium of 1–5 mL of high purity acetone was added.

After mechanical homogenization, the samples were pressed into tablets with a diameter of 5 mm at a pressure of approximately 2 Kbar using a hydraulic press. The pellets were then annealed at 600°C for 24 hours in sealed ampoules. This annealing temperature is optimal as it hardens the samples without significantly enlarging the grains of pyrrhotite and the phases formed by undissolved trace elements, as shown in our previous work.[14] The prepared pellets were then fixed into standard epoxy resin beads and polished using diamond pastes.

Instrumentation and operating conditions. The phase composition of the matrix pyrrhotite was examined using powder X-ray diffraction (XRD) on a Tongda TD-3700 (Cu-Kα, 1.54Å, 30 kV, 20 mA). The data processing was conducted utilizing the GSAS II software package.[15] Furthermore, the standard functions of GSAS II were utilized to determine the particle size of the powders from the profile parameters. Absolute crystallite sizes cannot be accurately determined without calibration standards. The data are presented as relative particle size ($D_{grinded}/D_{start}$) in order to demonstrate the size reduction that occurs during the milling process.

The grain morphology and concentration of the main components were determined using MIRA 3LMU (TESCAN, Czech Republic) and JSM 6510 LV (JEOL, Japan) scanning electron microscopes with an accelerating voltage of 20 kV.

The micro-homogeneity of the samples was checked by LA-ICP-MS method. All reference materials and samples were analyzed using identical line-scan parameters to ensure comparability. It is important to note that the instruments employed in such analyses can significantly influence the results obtained by this method. We obtained a good convergence of the results of the study, which was carried out on two quadrupole mass spectrometers:

The Thermo Xseries is equipped with a New Wave 213 laser attachment. The laser spot size was measured to be 60 μm, the scanning frequency was set to 15 Hz, the laser energy was calibrated to a range of 5-7 J/cm^2, and the scanning speed was configured to 10 μm/s. Prior to each analysis, a 30-second recording of the background signal was obtained. The material used for the ablation process was transported by helium flow (0.6 L/min) from the laser nozzle.

The Thermo Scientific iCAP Qc, accompanied by the NewWaveResearch laser attachment. The spot size of the ablation was measured at 50 μm, the pulse rate was set at 10 Hz, and the energy density was approximately 10 J/cm^2. The carrier gas comprised a mixture of helium (0.7 L/min) and argon (0.8 L/min). The scanning speed was 10 μm/s. Prior to each analysis, a 30-second recording of the background signal was obtained.

Subsequent processing of the data from both mass spectrometers demonstrated high convergence of the data. Concentrations were determined for the following isotopes: ^{33}S, ^{52}Cr, ^{55}Mn, ^{57}Fe, ^{59}Co, ^{60}Ni, ^{65}Cu, ^{66}Zn, ^{69}Ga, ^{72}Ge, ^{75}As, ^{77}Se, ^{95}Mo, ^{101}Ru, ^{103}Rh, ^{105}Pd, ^{107}Ag, ^{111}Cd, ^{113}In, ^{118}Sn, ^{121}Sb, ^{125}Te, ^{189}Os, ^{193}Ir, ^{195}Pt, ^{197}Au, and ^{208}Pb. Line profiles were obtained for each specimen, with durations extending up to 400 seconds. RSD

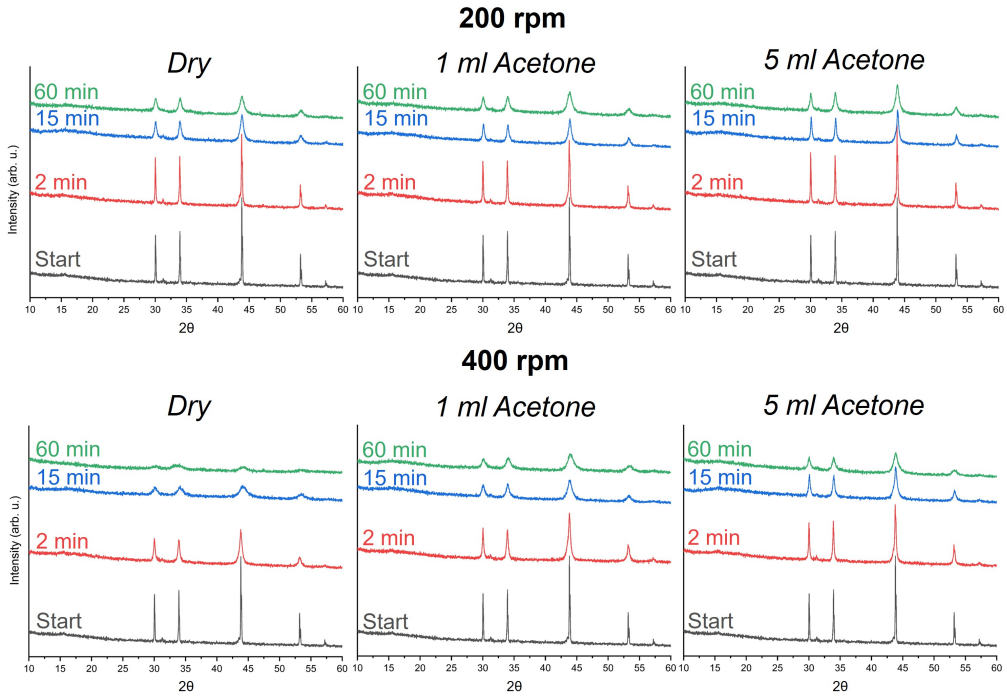

Fig. 1 The powder XRD patterns of pyrrhotite samples milled in a ball mill under varying conditions.

values were obtained by recalculating 1σ for each individual linear profile. The calculations were performed using LADR 1.1.7.0 and Iolite v2.5 software.[16] For calibration NIST610, UQAC FeS-1 and MASS-1[6, 17] materials were employed. Drift correction was performed using the ^{57}Fe internal standard with a fixed value of 62.32 weight %.

RESULTS AND DISCUSSION

Initially, the analysis of pyrrhotite powders milled under varying conditions was conducted by means of XRD (Fig. 1). It has been demonstrated that an increase in the rotation rate from 200 to 400 rpm results in a substantial enhancement in the grinding process. It was established that, irrespective of the rotational velocity or the presence or absence of a liquid medium, samples that underwent a grinding duration of two minutes exhibited no significant variation in their particle size when compared to the powder prior to the grinding process. As demonstrated by the experimental data, a notable decrease in the size of the particles is observed at the 15-min grinding point, which attains its maximum reduction at the 60-min point. It was found that an increase in the volume of liquid medium used led to a reduction in the degree of milling. The process of dry grinding was demonstrated to yield the smallest particles, down to the amorphous size, at the maximum rotation rate of 400 rpm.

Furthermore, all obtained powder diffraction patterns were refined by the Rietveld method to determine the mean crystallite size — not the agglomerate or particle size — of the powders after grinding, relative to unmilled powders with an initial particle size range of 1–10 μm. It should be noted that in mechanically activated systems such as these, individual particles often consist of multiple crystallites or may even approach amorphous character; thus, XRD-derived crystallite size does not directly equate to SEM-observed particle size. However, for the purpose of this study, crystallite size serves as a robust and reproducible proxy for tracking the progression of mechanical refinement over time, enabling quantitative comparison across milling regimes. The alterations in relative crystallite size as a function of milling time can be adequately approximated by an exponential relationship (Fig. 2). When grinding at 200 rpm, the relative crystallite size is unaffected by the presence or absence of a liquid medium. However, at 400 rpm, a marked difference becomes evident. In the context of a dry system, the relative crystallite size is observed to be minimal across all temporal ranges, with values of 8%, 3%, and 2% recorded for 2, 15, and 60 minutes of grinding, respectively. The incorporation of 1 mL of acetone resulted in an increase in relative crystallite size to 9%, 5%, and 3%, respectively, while the addition of 5 mL caused an increase to 14%, 7%, and 4%, respectively.

A comparison of the results of the approximated data from all experiments reveals that, commencing from 30–35 minutes, the

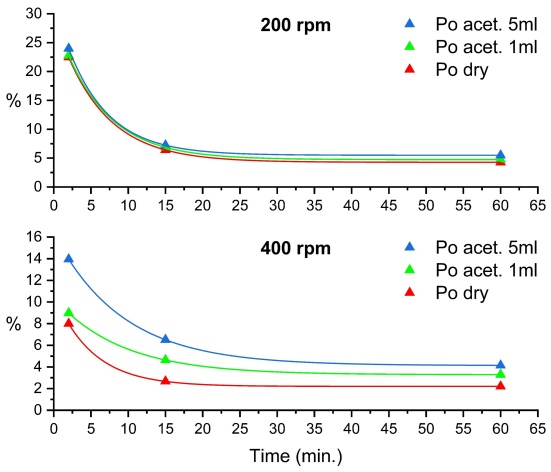

Fig. 2 Relative crystallite size (%) of pyrrhotite after planetary ball milling under different regimes, calculated from XRD peak broadening via Rietveld refinement.

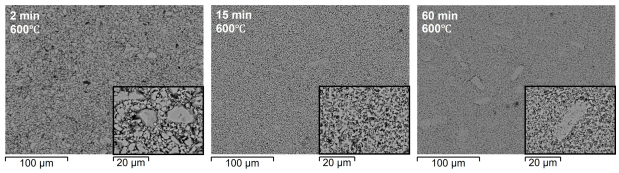

Fig. 3 BSE images of annealed at 600°C pyrrhotite samples after dry grinding at 200 rpm.

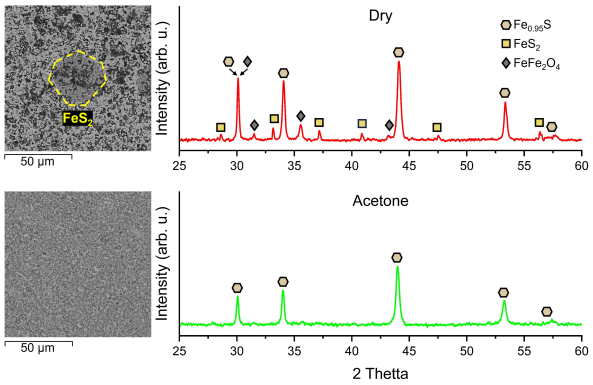

Fig. 4 BSE images of annealed at 600°C pyrrhotite samples after dry grinding at 200 rpm.

relative particle size remains virtually constant for each fixed set of varying grinding modes. It can be hypothesized that a subsequent reduction in particle size may be achieved by increasing the mill speed. However, 400 rpm is the upper operating limit of the instrument.

Following a grinding for additional homogenization of trace elements added and sintering, the pyrrhotite samples were annealed at 600°C and further analyzed by powder X-ray diffraction and SEM. The samples that were milled at 200 rpm for 2 min. were characterized by relatively coarse particle size (up to 20 µm) and significant porosity. After 15 min. of grinding, the particle size decreases to less than 5 µm. When grinding for 60 min, the particle size decreases to ~1 µm, but 'bean-shaped' agglomerates of ~10×30 µm are also formed (Fig. 3). Probably, when approaching the micron size of particles, their adhesion occurs at the moment of collision of grinding balls. Such spatial inhomogeneities can lead to a decrease in the homogeneity of impurity elements and are therefore highly undesirable. All samples did not show any multi-element inclusions, the 'nuggets' typical of sulfide and silicate standards.[12, 18-19] EDS analysis at random 20 points for each sample showed the matrix to be consistent with $Fe_{0.95}S$ pyrrhotite with a mean Fe:S ratio of 0.95 ± 0.02 (1σ). No secondary or trace phases were detected in any of the point and area for all the samples.

In the case of grinding at 400 rpm, pyrite (FeS_2) crystals measuring up to 50 µm in size were detected in all annealed samples after dry grinding (Fig. 4). Furthermore, powder XRD patterns of these samples also revealed the presence of magnetite ($FeFe_2O_4$). It is supposed that the detected phases are products of oxidation, occurring during grinding or due to interaction with air during powder extraction from the mill and pressing into tablets. Conversely, pyrite and magnetite were not detected in the annealed samples milled with acetone. For these samples the particle size was measured as less than 1µm for all milling rates used. Furthermore, these samples, as those prepared at 200 rpm, contain no 'nuggets', but also free of 'bean-shaped' agglomerates. Also, no deviations from $Fe_{0.95}S$ composition in measuring 20 points was detected.

The concentrations and homogeneity of trace elements in pyrrhotite samples grounded with 1 mL of acetone and annealed at 600°C were determined by LA-ICP-MS. In order to ascertain the effect of matrix compatibility on the calculations, calibration was performed using UQAC FeS-1 and MASS-1 sulfide standards and NIST 610 silicate standard. The results of the measurements are summarized in Table 1. The concentrations of most traces deviate significantly from those established during the sample preparation stage. One of the reasons for this discrepancy may be the error in weighting due to the difficulty of working with masses of the order of 10^{-3} g. However, if we assume that the weighting error is the only source of concentration discrepancy, then its value should be tens of percent, which is categorically impossible. In addition, for many elements, measured concentrations deviate both upward and downward from the expected concentrations depending on the standard used. In this case, we assume that the main factor of discrepancy may be the matrix effect caused by the difference of pyrrhotite matrix of samples and matrices of standards. This explains the particularly strong deviation of concentrations calculated from the silicate

Table 1. Results of LA-ICP-MS analyses of pyrrhotite samples obtained using NIST 610, UQAC FeS-1 and MASS-1 reference materials for the calibration

Element	Exp. conc.	NIST 610			UQAC FeS-1			MASS-1		
		Conc.	RSD	LOD	Conc.	RSD	LOD	Conc.	RSD	LOD
Cr	100	114.41	7.06	3.27	110.90	1.89	0.28	96.70	1.86	0.23
Mn	100	142.71	5.42	0.53	123.50	1.38	0.60	111.50	1.35	0.51
Co	100	321.45	7.04	0.07	259.40	1.50	0.02	217.20	1.50	0.01
Ni	100	755.93	7.36	1.39	777.00	2.25	0.26	541.00	2.31	0.19
Cu	101	221.68	7.20	0.97	160.20	2.90	0.08	131.80	2.88	0.07
Zn	101	414.75	1.66	1.68	232.00	3.23	0.15	185.00	3.24	0.11
Ga	100	149.82	7.52	0.09	68.40	2.34	0.04	85.10	2.35	0.05
Ge	100	112.51	2.09	0.86	-	-	-	29.40	2.21	0.06
As	44	98.14	3.17	3.92	49.50	1.72	0.14	42.40	1.77	0.12
Se	794	865.54	3.20	8.65	590.00	1.95	1.55	467.00	2.03	1.27
Mo	98	175.10	6.13	0.34	128.30	2.34	0.00	118.40	2.36	0.00
Ru	100	-	-	-	71.90	2.50	0.03	-	-	-
Rh	104	116.34	6.32	0.01	63.80	1.33	0.00	-	-	-
Pd	99	49.64	4.76	0.02	72.20	1.32	0.00	-	-	-
Ag	100	61.11	6.57	0.07	44.30	1.81	0.00	29.60	1.86	0.00
Cd	100	280.33	6.37	1.07	-	-	-	129.40	3.44	0.04
In	100	136.70	6.05	0.12	98.90	3.29	0.01	86.60	3.29	0.01
Sn	100	195.80	6.76	0.53	104.30	2.88	0.09	98.40	2.90	0.07
Sb	100	231.45	7.00	0.06	119.50	2.47	0.01	91.00	2.47	0.01
Te	771	161.90	4.17	0.97	71.40	2.38	0.31	57.40	2.44	0.28
Os	103	-	-	-	80.80	2.78	0.00	-	-	-
Ir	99	-	-	-	68.00	2.43	0.00	64.60	2.48	0.00
Pt	100	73.50	5.60	0.05	64.60	2.40	0.00	57.80	2.34	0.00
Au	101	108.49	9.42	0.04	61.70	2.11	0.01	58.90	2.12	0.01
Pb	100	153.48	6.37	0.04	122.50	1.63	0.01	110.40	1.63	0.01

Note:
Concentrations and LODs are given in ppm
A dash means that it is impossible to obtain data, i. e. due to the absence of an element in the reference material
Exp.conc. – expected concentration which was calculated from the masses of the added chalcogenides
RSD (1σ) is given as a percentage of the mean concentration

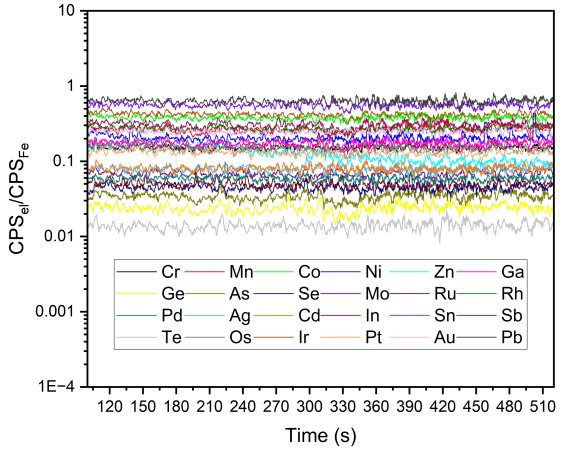

Fig. 5 Time resolved spectra of Fe normalized CPS in pyrrhotite from a LA-ICP-MS line scan across a distance of ~ 4000 μm using a spot size of 60 μm.

standard NIST 610, which is close in composition to window glass. Concurrently, the chemical compositions of MASS-1 and UQAC FeS-1 correspond to Fe-Zn-Cu and Fe-Ni-Cu, respectively. Consequently, the deviations in measured concentrations obtained using sulfide standards are comparatively minimal in comparison to those obtained using silicate NIST610. However, taking into account the divergent but similar trends of element concentrations obtained using all three standards, in this case we cannot deny the possibility of deviation of true concentrations from the estimated ones caused by migration of components during synthesis.

The results of the spatial homogeneity analysis are presented in the form of 1σ RSD. For the majority of elements, the RSDs calculated by MASS-1 and UQAC FeS-1 are within the range of 1-3%, indicating extremely high homogeneity. The results calculated by NIST610 are characterized by higher RSD values, which are in the range of 2-10%. This may be attributable to the comparatively low homogeneity of typical chalcophile elements in NIST 610.[20] An additional illustration of high homogeneity of trace elements in the obtained pyrrhotite are the time resolved spectra of Fe-normalized CPS for a profile with a length of about 4000 μm (Fig. 5). Even spectra without any anomalies are observed for all elements.

In order to ascertain the homogeneity of trace elements in the obtained pyrrhotite in the absence of the influence of external standards, the primary signals were processed as normalized to Fe. In multi-elemcent analysis employing LA-ICP-MS, there are several

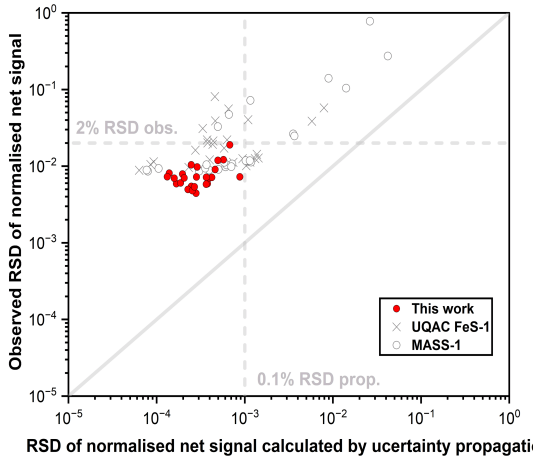

Fig. 6 Comparative analysis of the relative standard uncertainty of Fe normalized net signals, calculated from Poisson counting statistics only, and from the propagation of the uncertainty with those of observed values for Cr, Mn, Co, Ni, Cu, Zn, Ga, Ge, As, Se, Mo, Ru, Rh, Pd, Ag, Cd, In, Sn, Sb, Te, Os, Ir, Pt, Au, and Pb in pyrrhotite from this work, as well as UQAC FeS-1 and MASS-1. The solid grey line denotes a 1:1 correlation.

factors that can influence the resulting uncertainty. The elimination of correlated sources can be achieved through the process of internal standardization. Among the remaining uncorrelated sources, Poisson and flicker noise are significant. As flicker noise is ordinarily negligible at low concentrations and, consequently, signal levels, the Poisson distribution can be utilized to estimate the minimum uncertainty. [21-25] The relative standard uncertainty of Fe normalized net signals calculated from Poisson counting statistics only, and the observed uncertainties, were determined for pyrrhotite samples. A more detailed description of the calculation methods can be found in.[26] The results for pyrrhotite MASS-1 and UQAC FeS-1 are displayed in Fig. 6. The observed RSDs lie slightly above the Poisson limit (y=x line), indicating that minor real heterogeneity — not analytical noise — is the dominant source of variation. For all elements in pyrrhotite, the observed RSD signals are above the y=x line, indicating an additional source of uncertainty, which, for example, could be imperfect homogeneity. However, the values themselves are in close proximity to this straight line. For all elements in pyrrhotite, the observed RSDs of normalized signals are found to be no greater than 2%, and those calculated by Poisson statistics are 0.1%. Furthermore, the RSD values for pyrrhotite are lower than the values for MASS-1 and UQAC FeS-1, indicating its higher homogeneity.

CONCLUSION

The utilization of a planetary ball milling has been demonstrated to be a robust method for the production of sulfide powders with high homogeneity of trace elements. Nevertheless, the selection of the most appropriate milling regime is a pivotal factor. Pyrrhotite serves as a prime example of the limitations of the conventional homogenization technique involving grinding at maximum mill speed. In this instance, the most optimal method for pyrrhotite is grinding at 400 rpm in the presence of liquid (*e.g.* acetone), as this results in the smallest particle size and, consequently, the most uniform distribution of trace elements. Subsequent annealing of the obtained powder, which had been pressed into pellets, at 600°C provides the sulfide reference materials for LA-ICP-MS, which exhibited very high homogeneity (RSD ~2-3% for a 60 µm laser spot size) - already among the lowest reported for synthetic sulfide standards. While this level of homogeneity is sufficient for most analytical applications, further reduction in RSD may be achievable through systematic optimization of additional parameters, such as milling ball size and material, pressing pressure, use of iterative cycles of milling and annealing etc. Such refinements, though beyond the scope of this study, represent promising avenues for future research aimed at pushing the limits of microanalytical standards.

AUTHOR INFORMATION

Konstantin Kokh obtained his PhD (2008) and Doctor of Sciences (DSc, 2022) in Earth Sciences from the Institute of Geology and Mineralogy SB RAS, Novosibirsk, Russia. The scope of his research encompasses phase diagrams, crystal growth, the investigation of functional properties, and the practical applications of materials. He has published extensively, with a total of over 280 papers and an h-index of 35.

Corresponding Author

* K. A. Kokh

E-mail address: kokh@igm.nsc.ru

Notes

The authors declare no competing financial interest.

ACKNOWLEDGMENTS

AB acknowledges the Committee on Science of the Ministry of Science and Higher Education of the Republic of Kazakhstan (AP19576851) for its support in the mechanical activation of samples. X-ray diffraction analyses were done in Shared research facilities for multielemental and isotope study of the SB RAS under state assignment of IGM SB RAS 122041400031-2. The synthesis of materials and LA-ICP-MS analyses were supported by Russian Science Foundation (25-23-00155).

REFERENCES

1. M. Kelvin, E. Whiteman, J. Petrus, M. Leybourne, and V. Nkuna, *Miner. Eng.*, 2022, 176, 107322. https://doi.org/10.1016/j.mineng.2021.107322
2. Y. S. Liu, Z. C. Hu, M. Li, and S. Gao, *Chin. Sci. Bull.*, 2013, 58, 3863-3878. https://doi.org/10.1007/s11434-013-5901-4
3. P. Ouiya, D. Béziat, S. Salvi, G. Velásquez, S. Naba and A. Proietti, *Miner. Deposita*, 2025, 60, 1-20. https://doi.org/10.1007/s00126-024-01346-4
4. C. C. Wohlgemuth-Ueberwasser and K. P. Jochum, *J. Anal. At. Spectrom.*, 2015, 30, 2469-2480. https://doi.org/10.1039/C5JA00251F
5. C. Ballhaus and P. Sylvester, *J. Petrol.*, 2000, 41, 545-561. https://doi.org/10.1093/petrology/41.4.545
6. S. A. Wilson, W. I. Ridley, and A. E. Koenig, *J. Anal. At. Spectrom.,* 2002, 17, 406-409. https://doi.org/10.1039/B108787H
7. J. E. Mungall, D. R. Andrews, L. J. Cabri, P. J. Sylvester and M. Tubrett, *Geochim. Cosmochim. Acta.,* 2005, 69, 4349-4360. https://doi.org/10.1016/j.gca.2004.11.025
8. P. J. Sylvester, L. J. Cabri, M. N. Tubrett, G. McMahon, J. H.G. Laflamme and A. Peregoedova, Synthesis and evaluation of a fused pyrrhotite standard reference material for platinum group element and gold analysis by laser ablation-ICPMS //10th International Platinum Symposium: Oulu, Geological Survey of Finland, Extended Abstracts. 2005, 16-20. https://research.manchester.ac.uk/en/publications/synthesis-and-evaluation-of-a-fused-pyrrhotite-standard-reference
9. C. C. Wohlgemuth-Ueberwasser, C. Ballhaus, J. Berndt, V. Stotter née Paliulionyte, and T. Meisel, *Contrib. Mineral. Petrol*. 2007, 154, 607-617. https://doi.org/10.1007/s00410-007-0212-x
10. L. Ding, G. Yang, F. Xia, C. E. Lenehan, G. Qian, A. Mcfadden, J. L. Brugger, X. Zhang, G. Chen, and A. Pring, *Mineral. Mag.*, 2011, 75, 279-287. https://doi.org/10.1180/minmag.2011.075.2.279
11. P. Onuk, F. Melcher, R. Mertz-Kraus, H. E. Gäbler, and S. Goldmann, *Geostand. Geoanal. Res.*, 2017, 41, 263-272. https://doi.org/10.1111/ggr.12154
12. I. Belousov, L Danyushevsky, K. Goemann, S. Gilbert, P. Olin, J. Thompson, E. Lounejeva, and D. Garbe-Schönberg, *Geostand. Geoanal. Res.*, 2023, 47, 493-508. https://doi.org/10.1111/ggr.12512
13. L. Danyushevsky, P. Robinson, S. Gilbert, M. Norman, R. Large, P. McGoldrick, and M Shelley, *Geochem.: Explor. Environ. Anal.*,2011, 11, 51–60. https://doi.org/10.1144/1467-7873/09-244
14. A. O. Klimov, A. Bakhadur, V. D. Abramova and K. A. Kokh, *Microchem. J.*, 2025, 210, 112901. https://doi.org/10.1016/j.microc.2025.112901
15. B. H. Toby and R. B. Von Dreele, *J. Appl. Crystallogr.*, 2013, 46, 544-549. https://doi.org/10.1107/S0021889813003531
16. C. Paton, J. Hellstrom, B. Paul, J. Woodhead, and J. Hergt, *J. Anal. At. Spectrom.*, 2011, 26, 2508-2518. https://doi.org/10.1039/C1JA10172B
17. D. Savard, B. Bouchard-Boivin, S. Barnes, and D. Garbe-Schönberg, UQAC-FeS: A new series of base metal sulfide quality control reference material for LA-ICP-MS analysis. *Proceedings of the 10th International Conference on the Analysis of Geological and Environmental Materials*, Sydney, Australia, 2018, 8–13.
18. Y. Feng, W. Zhang, Z. Hu, Y. Liu, K. Chen, J. Fu, J. Xie, and Q. Shi, *J. Anal. At. Spectrom.*, 2018, 33, 2172-2183. https://doi.org/10.1039/C8JA00305J
19. M. Guillong, K. Hametner, E. Reusser, S. A. Wilson, and D. Günther, *Geostand. Geoanal. Res.*, 2005, 29, 315-331. https://doi.org/10.1111/j.1751-908X.2005.tb00903.x
20. K. P. Jochum, U. Weis, B. Stoll, D. Kuzmin, Q. Yang, I. Raczek, D. E. Jacob, A. Stracke, K. Birbaum, D. A. Frick, D. Günther, and J. Enzweiler, *Geostand. Geoanal. Res.*, 2011, 35, 397-429. https://doi.org/10.1111/j.1751-908X.2011.00120.x
21. J. Moser, W. Wegscheider, and T. Meisel, *J. Anal. At. Spectrom.*, 2003, 18, 508–511. https://doi.org/10.1039/B208746D
22. A. G. Adriaens, W. R. Kelly, and F. C. Adams, *Anal. Chem.*, 1993, 65, 660–663. https://doi.org/10.1021/ac00053a031
23. R. Hoelzl, C. Hoelzl, L. Kotz, and L. Fabry, *Accredit. Qual. Assur.*, 1998, 3, 185–188. https://doi.org/10.1007/s007690050219
24. A. T. Townsend, *Fresenius' J. Anal. Chem.*, 2000, 367, 614–620. https://doi.org/10.1007/s002160000416
25. C. P. Ingle, P. K. Appelblad, M. A. Dexter, E. J. Reid, and B. L. Sharp, *J. Anal. At. Spectrom.*, 2001, 16, 1076–1084. https://doi.org/10.1039/B103025F
26. Y. Luo, S. Gao, H. P. Longerich, D. Günther, S. Wunderli, H. L. Yuan, and X. M. Liu, *J. Anal. At. Spectrom.*, 2007, 22, 122-130. https://doi.org/10.1039/B608010C